Magnetocaloric effect in dipolar chains of magnetic nanoparticles with collinear anisotropy axes

D. Serantes,* D. Baldomir, and M. Pereiro
Departamento de Física Aplicada, Facultade de Física, Universidade de Santiago de Compostela, Campus Sur s/n, 15782 Santiago de Compostela, Spain

B. Hernando, V. M. Prida, and J. L. Sánchez Llamazares
Departamento de Física, Facultad de Ciencias, Universidad de Oviedo, Calvo Sotelo s/n, 33007 Oviedo, Spain

A. Zhukov, M. Ilyn, and J. González
Departamento Física de Materiales, Facultad de Química, UPV, 1072, 20080 San Sebastián, Spain
(Received 9 September 2009; published 27 October 2009)

We study the magnetocaloric effect (MCE) in parallel one-dimensional chains of dipole-dipole interacting magnetic nanoparticles with collinear magnetic anisotropy axes. By means of a Monte Carlo method we simulate the magnetic field dependence of the MCE for a field applied perpendicular to the anisotropy axes, finding the coexistence of direct and inverse MCE being both of reversible character. The inverse MCE-temperature range is quite small and progressively shifts to lower temperatures with increasing applied field until it disappears, thus we have mainly focused our study on the direct MCE-temperature range. We show the existence of a particular magnetic field value being proportional to the anisotropy field of the particles, $H^* \approx 2.5H_A$, which optimizes the magnetic entropy change and refrigerant capacity of the collinear aligned ensemble of nanoparticles.

DOI: 10.1103/PhysRevB.80.134421 PACS number(s): 75.30.Sg, 75.75.+a, 07.05.Tp, 75.30.Gw

I. INTRODUCTION

The fast nanotechnological miniaturization that is taking place nowadays requires the development of efficient cooling techniques able to work in such reduced dimensions.[1] Magnetic refrigeration (MR) using nanoscaled devices or materials constitute a promising choice to fulfill this requirement. MR is a friendly and green-saving environmental technology more efficient than conventional vapor-gas refrigerant technology.[2] Also, the unusual properties of nanosized materials compared to the bulk and their easier manipulating and assembling into different geometries make them attractive candidates for MR at the nanoscale.[3] MR is based on the magnetocaloric effect (MCE), the adiabatic temperature variation in a magnetic material under the application or removal of an external magnetic field.[4] The usual magnitude employed to evaluate the MCE is the variation in the magnetic entropy, ΔS_M, with the temperature. It can be calculated through the Maxwell's relation[5]

$$\Delta S_M(H,T) = \mu_0 \int_0^H \left(\frac{\partial M}{\partial T}\right)_{H'} dH'. \quad (1)$$

Both the magnetization **M** and the magnetic field **H** have to be treated as vectors to take into account the MCE originated from the rotation of the magnetic moment. To preserve the scalar form of Eq. (1), we will consider only the uniform magnetic field H and M will stand for the projection of the magnetization along the field direction.

From Eq. (1), we see that in order to have large MCE values for a given field $(\partial M/\partial T)$ should be large and for practical uses it is important to be able to tune these larger values in the appropriated temperature interval. In systems of magnetic nanoparticles, the shape of the thermomagnetic $M(T)$ curves and hence the magnitude of $(\partial M/\partial T)$ and its temperature position depends on a wide variety of factors of both internal (magnetic anisotropy and saturation magnetization)[6] and external origin (interparticle distances and magnetic field strength),[7] providing a rich scenario to obtain desired ΔS_M values. With an appropriate choice of the magnetic material,[6] spatial arrangement[8] and strength of the applied magnetic field,[9] it would be possible to tune the optimal magnetic properties of the system in order to reach a desired magnetocaloric response.

In this work we study the MCE in a nanoparticle system with enhanced magnetic anisotropy. The role played by the magnetic anisotropy on the MCE is getting a growing attention lately based on its importance for tailoring the magnetocaloric response of the system, as it has been recently reported for an ordered array of noninteracting oriented uniaxial magnetic objects under the effect of an external field H, perpendicularly applied respect to their easy-magnetization uniaxial anisotropy axes.[10] In this work we aim to go further by including also the magnetic dipolar interaction energy within the energies governing the magnetic behavior of the system. We have used a Monte Carlo (MC) technique to study the perpendicular-field dependence of the MCE in one-dimensional (1D) chains of dipolarly interacting monodisperse nanoparticles with collinear easy-anisotropy axes. This arrangement results in an enhanced anisotropy since the dipolar interaction favors the parallel alignment of the magnetic moments along the chains, adding to the nanoparticles' anisotropy energy. We have simulated *zero-field-cooling* (ZFC) and *field-cooling* (FC) magnetization curves as a function of the temperature for different magnetic field values perpendicularly applied to the aligned anisotropy axes, in order to study the MCE and evaluate its field dependence. We have found the coexistence of both direct and inverse MCE, in agreement with what is observed for the noninteracting case.[10] Furthermore, we show that

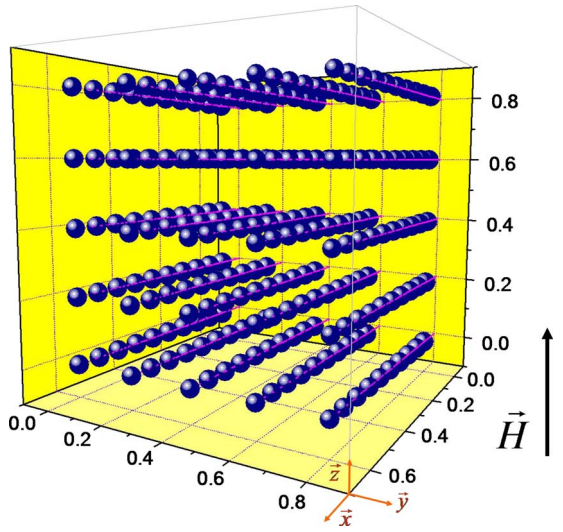

FIG. 1. (Color online) Schematic representation of the simulated system formed by an ordered array of 5×5 chains, each one with ten magnetic nanoparticles having their uniaxial anisotropy easy axes parallel aligned along the chains.

both direct and inverse MCE are of reversible character, very feasible attribute for MCE-based implementations, although the inverse MCE-temperature range is small and for this reason we have mainly focused our analysis on the direct MCE-temperature range. By analyzing the $(\partial M/\partial T)$ factor we have obtained that it reaches its maximum value at a particular field $H^*\approx2.5H_A$ (being H_A the anisotropy field of the particles), which stands for the field value that optimizes ΔS_M. To complete the MCE study we have also computed the refrigerant capacity (RC), i.e., the amount of heat able to be transferred between cold and hot sinks and that gives a more complete characterization of the MCE. Interestingly, we have found that it is also optimized at $H^*\approx2.5H_A$, which also supports the existence of a particular field optimizing the MCE.

II. COMPUTATIONAL DETAILS

We have used a MC method[6–9,14] to simulate the magnetic response of a system of magnetic nanoparticles spatially distributed in parallel 1D chains. The particles are supposed spherical and all of them equal in their characteristics, being well defined by its diameter d, uniaxial magnetic anisotropy constant K, and saturation magnetization, M_S. It is assumed monodomain particles with inner coherent rotation of the atomic magnetic moments. The magnetic moment of the i particle, which is proportional to its volume V_i, is defined as $|\vec{\mu}_i|=M_SV_i$. As illustrated in the Fig. 1, a well-ordered array of 5×5 chains is spatially distributed in a square net, every one composed of ten nanoparticles with their respective uniaxial anisotropy easy axes being parallel aligned along the chain length. The relative positions of the nanoparticles are $(x^*0.067, y^*0.200, z^*0.200)$, respectively.

The energies that characterize the nanoparticle system are Zeeman (E_H), anisotropy (E_A), and magnetic dipolar interaction (E_D). The coupling of a particle i to an external magnetic field H is written as

$$E_H^{(i)} = -\vec{\mu}_i\cdot\vec{H} \tag{2}$$

and for the uniaxial anisotropy we have

$$E_A^{(i)} = -KV\left(\frac{\vec{\mu}_i\cdot\hat{n}_i}{|\vec{\mu}_i|}\right)^2, \tag{3}$$

where $\hat{n}_i$ lies along the direction of the anisotropy easy axis. The magnetic dipolar energy between two particles i,j located at $\vec{r}_i,\vec{r}_j$, respectively, is given by

$$E_D^{(i,j)} = \left[\frac{\vec{\mu}_i\cdot\vec{\mu}_j}{r_{ij}^3} - 3\frac{(\vec{\mu}_i\cdot\vec{r}_{ij})(\vec{\mu}_j\cdot\vec{r}_{ij})}{r_{ij}^5}\right], \tag{4}$$

where r_{ij} is the interdistance between particles i,j.

The temperature dependence of those energies is computed to simulate the magnetic response of the system through the ZFC and FC thermomagnetic processes. The energy treatment is the same as followed in Refs. 6–9 and 14 but transferred to the current particular arrangement. We use the Metropolis algorithm applied to the individual movement of the magnetic moment of the nanoparticles: in every MC step (MC steps account for the simulation time), we select a particle at random and generate a new orientation of its magnetic moment. This new position is evaluated with probability $\min[1,\exp(-\Delta E/k_BT)]$, where k_B is the Boltzmann constant. The time is then incremented by N^{-1} so that in every MC step N attempts to change the configuration is made (N is equal to 250 for our particular system).

For the simulation procedure all the variables have been treated in normalized units, in such a way that the obtained results are general and easily translated into any other kind of particles characterized as above (monodisperse, spherical, and having uniaxial anisotropy). The normalized temperature is introduced as $t=k_BT/2KV$ while the applied magnetic field H is treated in terms of the normalized parameter $h=H/H_A$, related to the anisotropy field $H_A=2K/M_S$, and magnetization is normalized by the saturation value as $m=M/M_S$. However, in order to provide the reader a more intuitive idea about the discussed terms and results, ΔS_M and RC values have been expressed in unnormalized units. The characteristics of the particles used are $d=3.5$ nm, $M_S=541$ emu/cm^3, and $K=4.1\times10^5$ erg/cm^3 (similar to those of Ni nanoparticles).[11] The sample concentration is 5.8% volume fraction for this system.

The magnetic response of magnetic nanoparticle systems is highly time dependent, which is related to irreversible processes. Therefore it must be considered when studying magnetocaloric properties (for implementing a MCE-based refrigerating cycle the system must be reversible). To account for the time dependence of our system we have simulated the evolution of the magnetization with temperature through ZFC/FC processes, whose features are particularly adequate to differentiate reversibility in temperature, which is indicated by the overlapping of the two curves. To characterize the field dependence of the reversible MCE in our system, we have simulated ZFC/FC processes for different values of H. Both for the ZFC/FC curves the temperature variation ratio was $\Delta t=0.00245$ every 2000 MC steps and the results were obtained by averaging over 200 different configura-

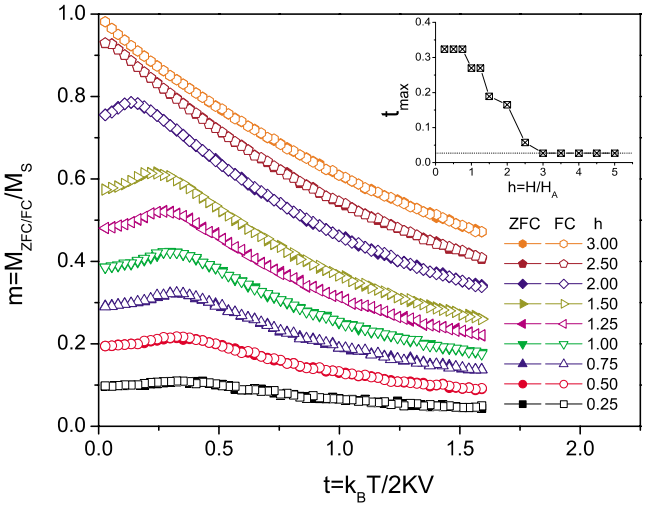

FIG. 2. (Color online) ZFC (full symbols) and FC (open symbols) $m(t)$ curves for different values of h. Inset shows t_{max} as a function of h.

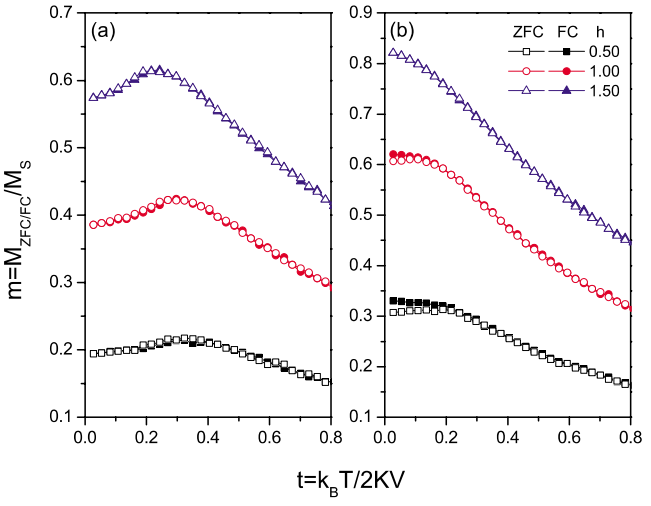

FIG. 3. (Color online) ZFC (full symbols) and FC (open symbols) $m(t)$ curves for the same values of h, both (a) for the collinear-easy-axes case and (b) for the random-easy-axes case.

tions. We show in Fig. 2 simulated ZFC/FC $m(t)$ curves for normalized magnetic field values in the range $0.25 \leq h \leq 3.00$.

The general trend of the ZFC/FC curves shown in Fig. 2 presents similarity with random anisotropy systems exhibiting superparamagnetism,[12] with the overlapping of the ZFC/FC curves at high temperatures, and the existence of a maximum (t_{max}) that progressively shifts its position toward lower values with increasing h.[9] However, remarkable differences with respect to the usual superparamagnetic behavior are observed illustrating a different physical origin. The maximum of the curves takes place for fields much larger than H_A, contrary to the expected disappearance of the peak for fields larger than H_A when t_{max} stands for the superparamagnetic blocking temperature.[13] This behavior is similar to that observed in randomly distributed particle systems at strong interacting conditions,[7] although we believe that in this particular case it might be related to other phenomena as a magnetic phase transition.[14] The ZFC/FC curves also coincide at low temperatures, contrary to the usual superparamagnetic behavior observed in random anisotropy systems in which the splitting between the ZFC and FC curves signals the blocked state of the particles. Meanwhile, the decrease in the FC curve below t_{max} with decreasing t instead of keeping growing as in superparamagnetic systems, points to an antiferromagneticlike arrangement of the system. These peculiar features arise from the particular orientation of the applied magnetic field with respect to the anisotropy axes of the nanoparticles. In usual superparamagnetic systems, the splitting between the ZFC and FC reflects the existence of local energy minima in the direction of the applied magnetic field. These minima originate by the magnetic anisotropy and represent stable energy wells that stand for different shapes of the $m(t)$ curves depending on the thermal history of the system. For particles with uniaxial anisotropy the most stable anisotropy well is the one that corresponds to parallel orientation of the magnetic moments with respect to the magnetic field, whereas the antiparallel case is less stable. It is this existence of the anisotropy wells what causes the irreversibility reflected in the divergence between the ZFC and FC curves: the different temperature trends followed in each process lead to different occupancies of the magnetic moments on the two energy wells and so to different thermomagnetization curves (until the thermal energy is large enough to overcome the anisotropy energy barrier between the minima). However, in our particular choose of the magnetic field direction perpendicularly applied to the easy-magnetization axes of the particles, none of the anisotropy wells is favored. Therefore, no irreversibility is generated and this is reflected in the coincidence of both the ZFC and FC curves. The decrease in the FC curve with decreasing t below t_{max} is also originated by the particular situation of the magnetic field applied perpendicular to the anisotropy axes and agrees quite well with the experimental behavior observed in systems having well-defined anisotropy easy axes under a perpendicularly applied magnetic field.[10] With the purpose to prove the above reasoning about the interplay between the orientation of the applied magnetic field with respect to the anisotropy easy axes as the origin of the features observed, we have simulated the same processes as in Fig. 2 but instead of collinear anisotropy axes case, by considering a random distribution of the easy axes for the array of nanoparticles. The ZFC and FC curves for some selected values of the applied field (h=0.50, 1.00, and 1.50, i.e., smaller, equal, and larger than the anisotropy field) are shown in Fig. 3 for giving a representative example of the arguments discussed above.

The noticeable differences between the collinear-easy-axes and the random-easy-axes cases represented in Figs. 3(a) and 3(b), respectively, clearly provide evidence supporting our arguments given above: the coincidence between the ZFC and FC curves corresponding to the collinear anisotropy case disappears when the uniaxial easy axes of nanoparticles are randomly distributed in which case the usual features of superparamagnetic systems are recovered. For a detailed study of the subjacent physical phenomena and the meaning of the maxima of the curves in the collinear anisotropy case

as related to a possible magnetic phase transition, see Ref. 14.

In connection with MCE, some features draw our attention. First, the coincidence of the ZFC and FC $m(t)$ curves in the whole temperature range, above and below t_{max}, proves the coexistence of both reversible normal (negative $\partial m/\partial t$ slope, above t_{max}) and inverse MCE (positive $\partial m/\partial t$ slope, below t_{max}). Therefore, we have demonstrated that the irreversible inverse MCE found in a randomly distributed interacting nanoparticle system at low temperatures[6] may be tuned into reversible character by controlling the magnetic anisotropy of the system. As we argued above, it is this specific orientation of the magnetic field, being perpendicularly applied with respect to the anisotropy easy axes, what accounts for the existence of reversible inverse MCE. Second, the slope of the curves for $t > t_{max}$ seems to rise with increasing fields in the considered ranges, what would account for larger MCE higher than the H_A limit for the disordered case.[8] For a complete characterization of the reversibility range and magnetic field dependence we have extended the simulations to fields up to 5.0 H_A. Inset in Fig. 2 shows the evolution of t_{max} as a function of h. It is observed that it progressively diminishes with increasing h, until it disappears for $h > 2.5$, further than the H_A limit for the superparamagnetic case.[13]

The temperature range accounting for the inverse MCE is short and of smaller slope than the direct MCE range. So, from now on we will focus our attention on the normal MCE-temperature range, in order to compare the results with those obtained in the random case. It remains as an interesting task for a future work about the study of how to extend the temperature operativeness of the inverse reversible MCE.

III. MAGNETOCALORIC PROPERTIES

In order to characterize the direct MCE in this peculiar system we have first analyzed by separate the value of $(\partial m/\partial t)$ as a function of h, with the purpose to check the possible existence of an optimizing magnetic field similar to that found in a randomly distributed particle system.[9] The results $(-\partial m/\partial t)$ vs h in the $t > t_{max}$ range where the system is reversible (and therefore in equilibrium) are plotted in Fig. 4.

It can be observed that the isofield curves exhibit a maximum, $(-\partial m/\partial t)_{max}$, that progressively shifts to lower temperature values with increasing field, attaining an absolute maximum value at $t \to 0$ for $h^* \sim 2.5$. For temperatures above the maximum the curves monotonically decrease, in a similar way as it was previously found in the random anisotropy case. However, although the general shape of the curves is similar to that observed in disordered systems the specific features completely differ. First, the value $t(-\partial m/\partial t)_{max}$ diminishes with increasing h, opposite to the disordered case.[9] Second, the absolute maximum takes place at an applied magnetic field value larger than the anisotropy field, H_A, of the particles, whereas for the disordered case it occurs at a field $h < 1$.

In Fig. 5 we represent both, $(-\partial m/\partial t)_{max}$ and $t(-\partial m/\partial t)_{max}$ vs h in detail. Two differentiated regimes are observed, at the transition marked by the particular field h^*

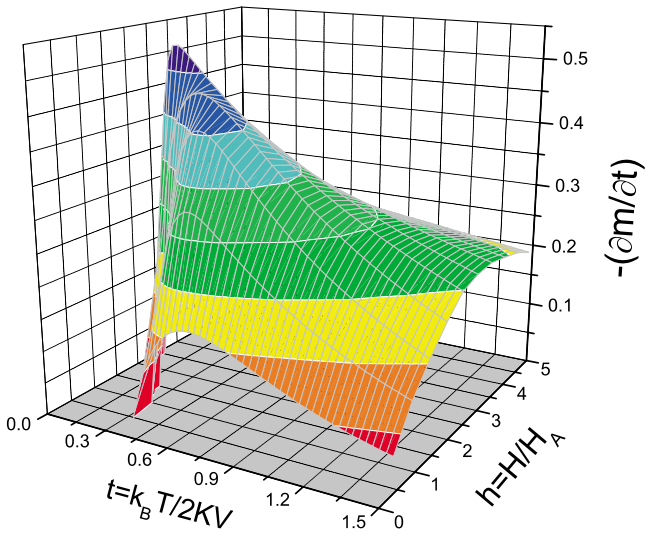

FIG. 4. (Color online) $(-\partial m/\partial t)$ vs h in the direct MCE reversible temperature range.

$= 2.5$. The $(-\partial m/\partial t)_{max}$ value grows with increasing field until it attains an absolute maximum at the particular value of $h^* = 2.5$, after which it decreases. This result is especially important for practical MCE implementation since it evidences the existence of a magnetic field value that optimizes the energy costs. The existence of a particular value of the magnetic field separating two ranges of behavior in both magnitudes had already been previously reported for disordered systems,[9] although at a much smaller value, around 0.3 H_A. This different behavior is important from the applied point of view since it allows setting the optimal magnetic field to larger fields. The temperature position of the maxima, $t(-\partial m/\partial t)_{max}$, rapidly decreases with increasing applied magnetic field h, following the opposite trend that in the random anisotropy case, where it rises with h.[9] For $h^* > 2.5$, it remains constant at the minimum temperature considered in the simulations. Finally, it is important to mention that the overall $(-\partial m/\partial t)$ values are considerably reduced in comparison with the random case. In this system $(-\partial m/\partial t)_{max} \approx 0.5$ while in the random case $(-\partial m/\partial t)_{max} \approx 1.5$, what in-

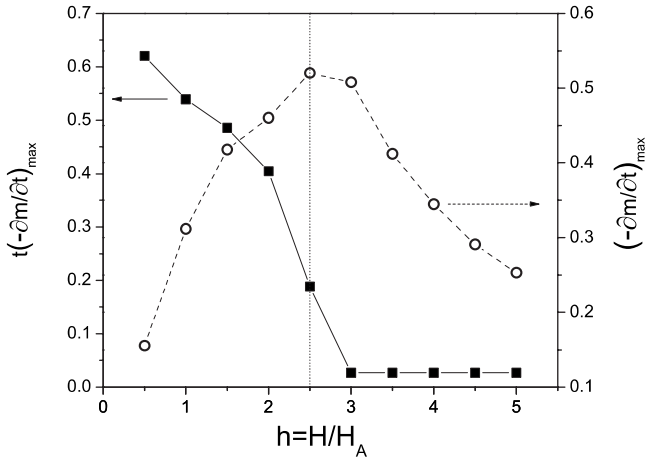

FIG. 5. Maximum $(-\partial m/\partial t)$ values and its temperature position, for the considered range of h values.

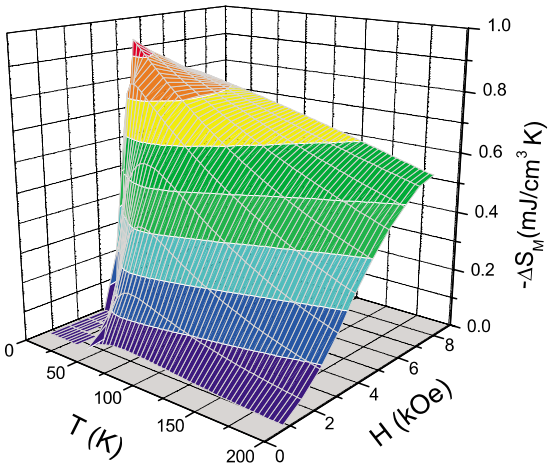

FIG. 6. (Color online) $-\Delta S_M$ hyperplane in the direct MCE reversible temperature range for different values of H.

dicates a better *a priori* adequacy of the random case for MCE-based implementations. As the MCE in magnetic nanoparticle systems depends much on the particle characteristics,[6] it constitutes the subject of a future work to evaluate the MCE in this spatial arrangement with other kinds of nanoparticles.

As it was previously mentioned in Sec. II, although the results here presented are applicable to any particle system with the assumed characteristics, we express the magnetocaloric parameters in unnormalized units to facilitate the interpretation to the reader. The nanoparticle characteristics used for the MCE simulations have been already described in Sec. II and to translate the results obtained from the previous sections into unnormalized units, it must be only necessary take into account that $M=mM_S$, $H=hH_A$, and $T=t2KV/k_B$. Figure 6 shows the ΔS_M values for the same cases as illustrated in Fig. 5 but using unnormalized magnitudes.

The overall shape of the ΔS_M hyperplane displayed in Fig. 6 exhibits two different tendencies depending on the temperature range. For high temperatures, ΔS_M monotonically increases with H, although the growing ratio diminishes above intermediate fields (for intermediate fields we mean values of the order of the h^* obtained in Fig. 7). At low temperatures the curves exhibit a peak, as expected from the results discussed in Figs. 3 and 4.

For a real MCE-based implementation, as much important as having high values of ΔS_M it matters the temperature range at which those values are attained. For a complete characterization of the MCE it is usually also computed the RC as we mentioned earlier. The RC is a parameter that takes into account the shape of the ΔS_M curves, computing the amount of heat that the material is able to transfer in a thermodynamic cycle for a given field change ΔH between the working temperatures of cold and heat sinks, T_{cold} and T_{hot}, respectively. It can then be evaluated as

$$\mathrm{RC} = \int_{T_{cold}}^{T_{hot}} [\Delta S_M(T,H)]_{\Delta H} dT. \quad (5)$$

The temperatures T_{cold} and T_{hot} are usually evaluated as the temperatures at half maximum of the $\Delta S_M(T)$ curve.

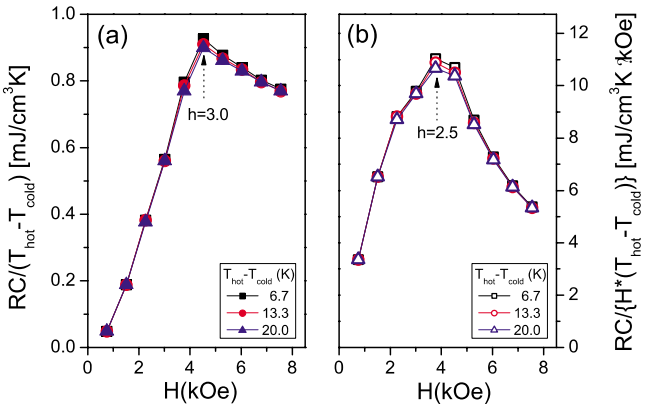

FIG. 7. (Color online) RC as a function of h, normalized (a) by the WTR and (b) by the WTR$\times h$.

However, in our system the curves are very flat and would account for a wide temperature range not very representative of the obtained values. Therefore, instead of evaluating the RC for different working temperature ranges (WTR$=T_{hot}-T_{cold}$) we normalized it as RC/WTR, in order to evaluate its potentiality as a heat transfer. The results for the WTR values of 6.7, 13.3, and 20.0 K are displayed in Fig. 7.

In Fig. 7(a), it can be observed that RC remains practically unchanged for the different WTR considered values. The overall shape continuously increases until $h=3.0$, followed by a further decrease. For the nanoparticles here considered, this value stands for a magnetic field $H=4.542$ kOe. It is very important for real applications to optimize the energy necessary to implement a MR cycle, which is the energy necessary to generate the magnetic field. Therefore we have also analyzed the previous value normalized by the magnetic field, being plotted in Fig. 7(b). It is obtained a maximum at the particular value of $h=2.5$, the same value that maximizes $\partial m/\partial t$. For the particles we consider here, $H_A=1.514$ kOe, and therefore the field that optimizes RC is $H=3.785$ kOe.

Finally, we compare the present results with some MCE studies recently reported in other nanosized systems. Although the results obtained were expressed in volumetric units to give an useful estimation from the applied point of view,[4] it is commonly found in the literature the use of mass units J kg^{-1} K^{-1}, therefore we also express the results in these same units for comparison. To translate the values to this scale it is only necessary to know the volume density and in our case we take the Ni bulk density, $\rho=8.9$ g/cm^3. The largest values obtained, in the low-temperature limit and for a field change of 3.8 kOe, correspond in mass units to $\Delta S_M=0.105$ J/kg K and RC$=2.0$ J/kg. The maximum ΔS_M is about one order the magnitude larger than the ones found in ferrite nanoparticles[3] and only one order of magnitude smaller than the large cryogenic MCE recently reported in the low-temperature limit for magnetic nanocapsules if normalized by the magnetic field: in our system $\Delta S_M=0.27$ J/kg K T while for magnetic nanocapsules as $TbAl_2$, graphite-coated Gd, and $GdAl_2$ (Refs. 15–17, respectively), $\Delta S_M=3.04$, 8.13, and 2.90 J/kg K T. In general, both the ΔS_M and RC values are around two orders of magnitude smaller than the reported for the best bulk magnetocaloric

materials[3] when normalizing with the magnetic field.

Good candidates to exhibit such novel phenomena described in this work, particularly the reversible character of the inverse MCE, are, in general, systems with a well defined and collinear anisotropy easy axis. Those characteristics may be found in a wide variety of systems, ranging from the ferromagnetic nanowires reported in Ref. 10 to large arrays of nanostructured ferromagnets as those reported in Ref. 18. Using magnetic nanoparticles, the most promising candidates at the moment are FePt systems, whose large anisotropy allows a quite good (although not complete yet) alignment of the anisotropy easy axes (see, for example, Refs. 19 and 20).

IV. CONCLUSIONS

We have used a MC technique to study the MCE in parallel chains of dipolarly interacting magnetic nanoparticles with collinear anisotropy axes. The magnetostatic dipolar interaction energy favors the parallel alignment of the magnetic moments of the nanoparticles along the chains, which results in an enhancement of the anisotropy. This anisotropic system exhibits a magnetic response under the perpendicular application of a magnetic field H respect to the anisotropy easy axis quite similar to superparamagnetism, with a similar overall shape of the curves and exhibiting a maximum of magnetization that shifts to lower temperatures with increasing H, although also presents different features suggesting different physical origin. We have found the coexistence of direct (above the maximum) and inverse (below the maximum) MCE both of reversible character, although the inverse MCE-temperature range is small and disappears with increasing the field, therefore it must be extended to become of practical use. Therefore we focused our analysis mainly in the direct MCE-temperature range. The detailed analysis of the $(-\partial m/\partial t)$ factor in this range reveals the existence of a maximizing field $H^* \approx 2.5H_A$, which optimizes ΔS_M and accounts so for an optimal MCE. We have also evaluated the RC and found that it is practically temperature independent up to 20K and it is also optimized at the same field $H^* \approx 2.5H_A$, which reinforces the adequacy of using this particular field to optimize the MCE for such nanostructured magnetic nanoparticle systems.

ACKNOWLEDGMENTS

We thank the Xunta de Galicia (XdeG), Project INCITE 08PXIB236052PR, and the Spanish Ministry of Education and Science under Projects No. MAT2006-10027, No. MAT2006-13925-C02-01, No. MAT2009-13108-C02-01, No. MAT2009-08165, No. NAN2004-09203-C04-03, No. NAN2004-09203-C04-04, and FICYT under Projects No. FC04-EQP-28 and IB09-131. We thank the Centro de Supercomputación de Galicia (CESGA) for computational facilities. D. Serantes and M. Pereiro also acknowledge XdeG for financial support (Maria Barbeito and Isabel Barreto programs, respectively). FICYT is acknowledged by J. L. Sanchez Llamazares (Contract No COF07-013).

*david.serantes@usc.es

[1] J. Gass, H. Srikanth, N. Kislov, S. S. Srinivasan, and Y. Emirov, J. Appl. Phys. **103** 07B309 (2008).
[2] O. Tegus, E. Brück, K. H. J. Buschow, and F. R. de Boer, Nature (London) **415**, 150 (2002).
[3] P. Poddar, J. Gass, D. J. Rebar, S. Srinath, H. Srikanth, S. A. Morrison, and E. Carpenter, J. Magn. Magn. Mater. **307**, 227 (2006).
[4] K. A. Gschneidner, Jr., V. K. Pecharsky, and A. O. Tsokol, Rep. Prog. Phys. **68**, 1479 (2005).
[5] H. B. Callen, *Thermodynamics* (Wiley, New York, 1981), Chap. 14.
[6] D. Serantes, D. Baldomir, M. Pereiro, J. Botana, V. M. Prida, B. Hernando, J. E. Arias, and J. Rivas, J. Nanosci. Nanotechnol. (to be published).
[7] D. Serantes, D. Baldomir, M. Pereiro, J. E. Arias, C. Mateo-Mateo, M. C. Buján-Núñez, C. Vázquez-Vázquez, and J. Rivas, J. Non-Cryst. Solids **354**, 5224 (2008).
[8] D. Baldomir, J. Rivas, D. Serantes, M. Pereiro, J. E. Arias, M. C. Buján-Núñez, and C. Vázquez-Vázquez, J. Non-Cryst. Solids **353**, 793 (2007).
[9] D. Serantes, D. Baldomir, M. Pereiro, J. Rivas, C. Vázquez-Vázquez, M. C. Buján-Núñez, and J. E. Arias, Phys. Status Solidi A **205**, 1349 (2008).
[10] V. Franco, K. R. Pirota, V. M. Prida, A. Neto, A. Conde, M. Knobel, B. Hernando, and M. Vazquez, Phys. Rev. B **77**, 104434 (2008).
[11] D. Gozzi, A. Latini, G. Capannelli, F. Canepa, M. Napoletano, M. R. Cimberle, and M. Tropeano, J. Alloys Compd. **419**, 32 (2006).
[12] S. Bedanta and W. Kleemann, J. Phys. D **42**, 013001 (2009).
[13] R. H. Victora, Phys. Rev. Lett. **58**, 1788 (1987).
[14] D. Serantes, D. Baldomir, M. Pereiro, B. Hernando, V. M. Prida, J. L. Sánchez Llamazares, A. Zhukov, M. Ilyn, and J. González, J. Phys. D: Appl. Phys. **42**, 215003 (2009).
[15] X. G. Liu, D. Y. Geng, J. Du, S. Ma, B. Li, P. J. Shang, and Z. D. Zhang, Scr. Mater. **59**, 340 (2008).
[16] X. G. Liu, D. Y. Geng, Q. Zhang, J. J. Jiang, W. Liu, and Z. D. Zhang, Appl. Phys. Lett. **94**, 103104 (2009).
[17] S. Ma, D. Geng, W. Zhang, W. Liu, X. Ma, and Z. Zhang, Nanotechnology **17**, 5406 (2006).
[18] C. Teichert, J. Barthel, H. P. Oepen, and J. Kirschner, Appl. Phys. Lett. **74**, 588 (1999).
[19] S. Kang, Z. Jia, S. Shi, D. E. Nikles, and J. W. Harrell, Appl. Phys. Lett. **86**, 062503 (2005).
[20] Z. Jia, S. Kang, S. Shi, D. E. Nikles, and J. W. Harrell, J. Appl. Phys. **99**, 08E904 (2006).